

Journal of Biomedical Optics

SPIEDigitalLibrary.org/jbo

Intravital microscopy of subpleural alveoli via transthoracic endoscopy

David Schwenninger
Hanna Runck
Stefan Schumann
Jörg Haberstroh
Sven Meissner
Edmund Koch
Josef Guttmann

Intravital microscopy of subpleural alveoli via transthoracic endoscopy

David Schwenninger,^a Hanna Runck,^a Stefan Schumann,^a Jörg Haberstroh,^b Sven Meissner,^c Edmund Koch,^c and Josef Guttman^a

^aUniversity Medical Center Freiburg, Division of Experimental Anaesthesiology, Hugstetter Strasse 55, 79106 Freiburg, Germany

^bUniversity Medical Center Freiburg, BioMed Center, Experimental Surgery, Hugstetter Strasse 55, 79106 Freiburg, Germany

^cUniversity of Technology Dresden, Clinical Sensing and Monitoring, Medical Faculty, Fetscherstrasse 74, 01307 Dresden, Germany

Abstract. Transfer of too high mechanical energy from the ventilator to the lung's alveolar tissue is the main cause for ventilator-induced lung injury (VILI). To investigate the effects of cyclic energy transfer to the alveoli, we introduce a new method of transthoracic endoscopy that provides morphological as well as functional information about alveolar geometry and mechanics. We evaluate the new endoscopic method to continuously record images of focused subpleural alveoli. The method is evaluated by using finite element modeling techniques and by direct observation of subpleural alveoli both in isolated rat lungs as well as in intact animals (rats). The results confirm the overall low invasiveness of the endoscopic method insofar as the mechanical influences on the recorded alveoli are only marginal. It is, hence, a suited method for intravital microscopy in the rat model as well as in larger animals. © 2011 Society of Photo-Optical Instrumentation Engineers (SPIE). [DOI: 10.1117/1.3560297]

Keywords: intravital microscopy; alveoli; endoscopy; frequency domain optical coherence tomography; lungs; imaging.

Paper 10533R received Oct. 1, 2010; revised manuscript received Feb. 7, 2011; accepted for publication Feb. 8, 2011; published online Apr. 1, 2011.

1 Introduction

Since it was clinically proven, for the first time in 2000, that ventilatory settings influence patient mortality,¹ development of lung-protective ventilation strategies to prevent ventilator-induced lung injury (VILI)² came to be a focus of interest in intensive care medicine. Because VILI develops on the alveolar level,³ understanding of alveolar mechanics is crucial in the process of developing lung-protective ventilation strategies. For intravital analysis of mechanical tissue properties such as lung tissue mechanics, we recently introduced a method based on endoscopic microscopy.⁴ In addition to this functional information about lung tissue mechanics, the same endoscopic method provides morphological information about the intrabreath cyclic changes of alveolar geometry. There have already been many studies that used experimental methods to optically track alveoli in mechanically ventilated animals, including the pioneering works of Nieman's group.⁵⁻¹¹ However, because the results of some of these studies are inconsistent, there is still the need for further observations. Hence, new methods for intravital imaging of subpleural alveoli have recently been presented.¹²⁻¹⁵

A methodological problem for alveolar imaging arises from the cyclic expansion and contraction of the lung during mechanical ventilation, causing in- and out-of-focus movement of the alveoli in the microscopic field of view. If identical alveoli are wished to be continuously optically tracked during complete respiratory cycles, then fixation of the alveolar parenchyma, at least in the focus plane, is necessary. Furthermore, most existing

methods of intravital microscopy (IVM) require removing relevant parts of the thoracic wall, which may influence respiratory system mechanics.

We describe and evaluate a new IVM method that provides adjustable local mechanical fixation for keeping in-focus the alveolar tissue being under observation. The method does not require removing the thoracic wall, thus allowing for free movement of the lung. It is based on an endoscopic system^{4,16} that is inserted into the thoracic cavity through intercostal space. In this study, we evaluated the endoscopic IVM method, theoretically, by means of finite element (FE) models and, practically, by applying our method on isolated rat lungs and on lungs in intact rats (*in vivo*). We hypothesized that the transthoracic endoscopy does not affect local alveolar and global lung mechanics in the sense of minimal invasiveness.

2 Methods

2.1 Endoscopic System

The endoscopic system consists of a rigid endoscope (Schöllly Fiberoptic GmbH, Denzlingen, Germany) inserted in two concentric trocars (6.5 mm o.d., Fig. 1). The system was designed to guide a controlled fluidic flow from the outer toward the inner trocar to create a defined negative pressure (p_{Tip}) at its tip (described in detail elsewhere⁴).

2.2 Model-Based Evaluation

FE model I (Fig. 1) of the endoscopic system was used to evaluate the pressure distribution at the site of contact between

Address all correspondence to: David Schwenninger, University Medical Center Freiburg, Division of Experimental Anaesthesiology, Hugstetter Strasse 55, Freiburg, BW 79106 Germany. Tel: 0049 (0)761 270 2308; Fax: 0049 (0)761 270 2328; E-mail: David.Schwenninger@uniklinik-freiburg.de

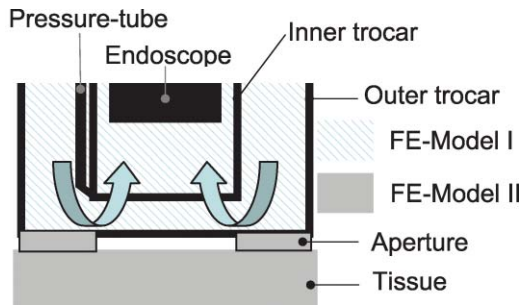


Fig. 1 Schematic view of the endoscopic system's tip. The endoscopic system consists of the endoscope concentrically embedded in a two-trocar system, including a pressure tube for pressure measurement. The outer trocar ends with an aperture through which the investigated tissue can be observed via the endoscope. By liquid flow, directed from the outer to the inner trocar (arrows), negative pressure can be applied. Shadings indicate compartments that were simulated by FE model I (modeling laminar flow and resulting pressure). The gray areas were included in the FE model II (modeling stress and strain caused by the pressure in the field of view).

endoscope and alveolar tissue. Laminar flow was modeled using the FE modeling software COMSOL (version 3.5a, COMSOL Multiphysics GmbH, Göttingen, Germany). The modeled fluid input was kept at constant pressure and the output at constant flow so that the mean pressure at the tip of the endoscopic system was negative.

FE model II (Fig. 1) was created to assess the stress and strain distribution in a soft elastic material when negative pressure is applied on it by the endoscopic system. Material properties of the model were based on data results from Ref. 4 (shear modulus = 4.5 kPa and bulk modulus of air = 100 kPa).

2.3 Evaluation in Isolated Lung

To evaluate the optical image quality of the endoscopic system, recordings of subpleural alveoli from isolated rat lungs were compared to recordings of an established method for combined darkfield (DF) microscopy and frequency-domain optical coherence tomography (FDOCT).¹³ Images were recorded at constant intrapulmonary pressures of 7 and 12 mbar. The same area of subpleural alveoli was recorded by means of all three methods. Subsequently, the images were manually matched to find identical structures in the different recordings. The outlines of matched alveoli were manually marked in the images of endoscopic microscopy, and the surficial areas of the alveoli were computed. For comparison, the relative differences in surficial area of identical alveolar structures were calculated from DF microscopy and endoscopy images.

2.4 Evaluation In Vivo

For method evaluation under *in vivo* conditions, the endoscopic method was used in a rat model (28 Wistar-rats; Charles River, Sulzfeld, Germany). The experiments were approved by the local ethics committee and were carried out according to the guidelines on the ethical use of animals.

To quantify the influence of the endoscopic system on the cardiovascular system, we measured mean arterial blood pressure (MAP) and partial arterial oxygen pressure (paO_2). To estimate the method's influence on the respiratory system, two respiratory

manoeuvres were designed: (i) low-flow manoeuvre: increase of pressure from 3 to 40 mbar within 5 s followed by a 5-s pressure decrease back to 3 mbar and (ii) PEEP-wave manoeuvre: stepwise increase of the positive end expiratory pressure (PEEP) by 3 mbar from 0 to 15 mbar and back to 0 again. As a quantitative measure for method's influence on the respiratory system, the dynamic compliance¹⁷ was determined for different PEEP levels of the PEEP-wave.

2.5 Protocol

Rats were anesthetized, tracheotomised, and tracheally intubated. Subsequently, volume-controlled ventilation was applied via a small animal ventilator (FlexiVent, Scireq, Montreal, Canada). Ventilation was started with 70 breaths per minute, tidal volume of 10 ml/kg bodyweight and PEEP of 2 mbar. Arterial blood pressure was measured invasively via a catheter placed in the *arteria carotis communis*. Inspiratory and expiratory gas flows were measured via two separate flow sensors (Fleisch 000, Dr. Fenyves und Gut GmbH, Hechingen, Germany). Pressure and flow values were recorded using custom software.

The rats were randomly distributed to the control or the lung injury group. Lung injury was induced via bronchoalveolar lavage with physiological saline solution.¹⁸ Thereby, surfactant was washed out. The lavage procedure was repeated with 15 ml of liquid per kilogram bodyweight until blood gas analysis showed a Horowitz Index ($\text{paO}_2/\text{FiO}_2$) of <200 mmHg, which is a criterion for acute respiratory distress syndrome.¹⁹ As a sham manoeuvre, the control group was ventilated mechanically for an equivalent time.

After induction of injury/sham, ventilation was continued for 20 min at a PEEP level of 7 mbar. Subsequently, the intercostal space between the fifth and sixth rib was opened dorsally at the left side of the thorax (in each animal at the same position relative to the dorso-ventral axis) and a trocar for guiding the endoscopic system was inserted. This trocar was anchored inside the thorax between the ribs and fixed with a screw nut from outside of the thorax. Hence, the aperture allowed inserting the endoscopic system into the thorax cavity. The animal was then placed in supine position, and the endoscopic system was inserted through the trocar until its tip touched the surface of the lung. The pressure in the endoscope's field of view (p_{Tip}) was then adjusted so that subpleural alveoli stayed in focus during ventilation (average pressure = -3 mbar). After insertion, ventilation was continued for 5 min at a PEEP of 7 mbar.

Measurement manoeuvres were performed, blood-gases were analyzed, and the MAP was noted before and after placement of the endoscopic system. At the end of the protocol, the rat was killed by exsanguination.

2.6 Influence of Fixation

To determine the influence of p_{Tip} on the alveolar size, p_{Tip} was ramped from -3 mbar to -30 mbar at constant airway pressures of 30, 15, 20, and 17 mbar. The optical change in the size of alveoli due to their movement toward the endoscope's tip due to the negative p_{Tip} was thereby compensated for by reference measurement of the size of spherical ceramic particles that touched the lung's surface (method described in detail elsewhere⁴). Any movement of the subpleural alveoli toward

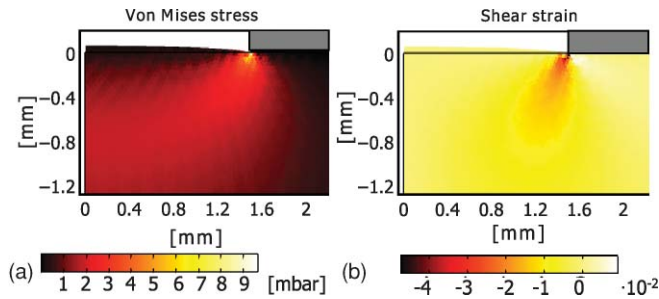


Fig. 2 FE model II of strain and stress distribution inside a material observed using the endoscopic system (stress and strain due to negative pressure of -3 mbar). The left border is the rotational symmetry axis. (a) Von Mises stress (absolute value of stress inside the tissue) and (b) global shear strain.

the endoscope's tip due to the negative p_{Tip} results in an optical enlargement of alveoli and particles in the video.⁴ However, the negative p_{Tip} could lead to a physical enlargement of the alveoli but not of the particles. The relative change in alveolar area was divided by the relative change in particle area to retrieve the change in physical alveolar size [$\Delta A(p_{\text{Tip}})$].

3 Results

Analysis of the fluidic pressure relationships inside the trocar system (FE model I) revealed that the highest pressure across the circular opening on the endoscopic system's tip is in its center and the lowest pressure is at its edge. The relative pressure difference between center and edge was 1.82% of the mean pressure.

Modeling an observed tissue (FE model II) revealed that the stress inside the subpleural alveolar tissue (~ 100 μm under the tissue-surface) is considerably lower than the applied p_{Tip}

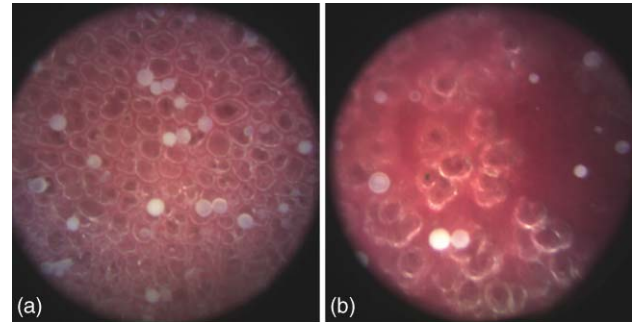


Fig. 4 Subpleural alveoli recorded with the endoscopic system *in vivo*. Images show representative video frames from (a) a control animal and (b) an animal with lung injury. The ceramic particles are visible as white circles.

(Fig. 2). The calculated shear strain in this layer was close to zero.

Images from identical alveolar structures of isolated lungs obtained from the three imaging methods recorded at intrapulmonary pressures of 7 and 12 mbar have been matched (Fig. 3). The matched structures were comparable with respect to shape and size. The relative difference of the alveoli's area size in images resulting from the endoscopic system and the DF microscope was $2.5 \pm 6.3\%$ (mean \pm SD). Subpleural alveoli were successfully recorded *in vivo* in rats with healthy and injured lungs (Fig. 4). Of the 28 examined rats, data from four were excluded due to death prior to the end of the protocol, leaving data from 13 animals from the control group and 11 from the lung injury group. paO_2 was never influenced from insertion of the endoscope (Table 1). In the lung-injured rats, dynamic compliance (C) was never influenced by insertion of the endoscope. In contrast, in the healthy group, C measured after increasing PEEP but not after decreasing PEEP was significantly reduced after insertion of the endoscope. Two-way analysis of variance

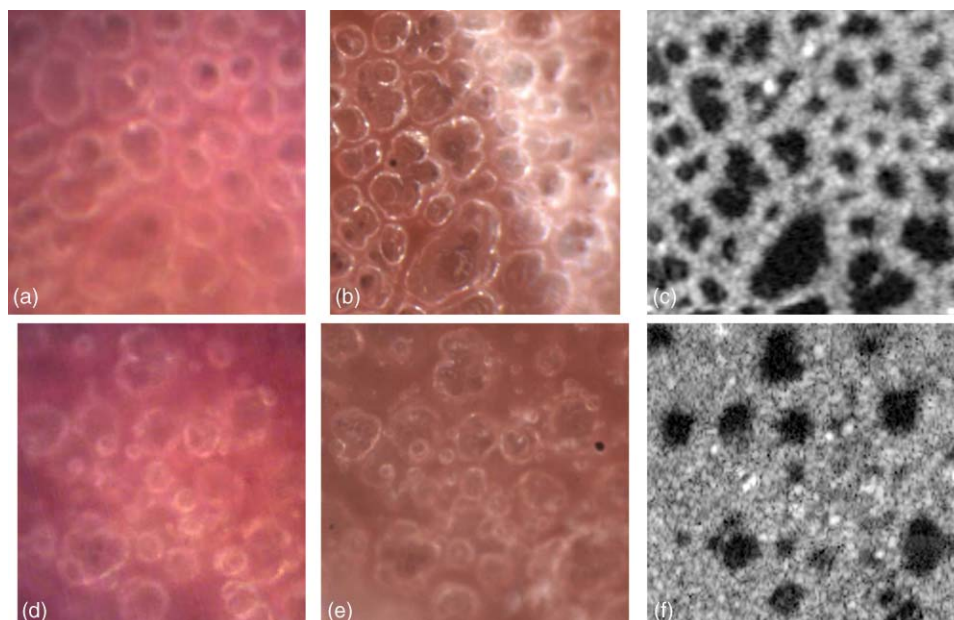


Fig. 3 Identical subpleural alveoli of isolated lungs recorded with (a,d) the endoscopic system, (b,e) the DF microscopy, and (c,f) the FDOCT. (a–c) were recorded at constant airway pressure of 12 mbar, (d–f) at 7 mbar.

Table 1 Data (mean \pm SD) for control and lung injury group. Data are compared before and after endoscope insertion. *p*-values from Student's *t*-tests are given as a measure of significance of the differences. MAP: mean arterial blood pressure; *paO*₂: partial arterial O₂ pressure; and *C*: dynamic respiratory system compliance at the following PEEP-levels: 3 and 9 mbar while PEEP was increased (\uparrow) and while PEEP was decreased (\downarrow) and 15 mbar (maximum PEEP).

		MAP [mmHg]	<i>paO</i> ₂ [mmHg]	<i>C</i> (ml/mbar) \uparrow PEEP 3	<i>C</i> (ml/mbar) \uparrow PEEP 9	<i>C</i> (ml/mbar) PEEP 15	<i>C</i> (ml/mbar) \downarrow PEEP 9	<i>C</i> (ml/mbar) \downarrow PEEP 3
Control	Before	69 \pm 11	561 \pm 36	0.58 \pm 0.1	0.61 \pm 0.12	0.6 \pm 0.11	0.41 \pm 0.2	0.27 \pm 0.11
	After	67 \pm 19	547 \pm 43	0.44 \pm 0.1	0.47 \pm 0.15	0.43 \pm 0.1	0.35 \pm 0.12	0.28 \pm 0.1
	<i>p</i> -Value	0.8	0.3	0.0012	0.011	0.0004	0.37	0.85
Injury	Before	61 \pm 6	130 \pm 43	0.34 \pm 0.07	0.3 \pm 0.07	0.29 \pm 0.05	0.23 \pm 0.05	0.22 \pm 0.06
	After	52 \pm 9	112 \pm 39	0.32 \pm 0.09	0.3 \pm 0.09	0.27 \pm 0.08	0.23 \pm 0.05	0.22 \pm 0.1
	<i>p</i> -Value	0.026	0.48	0.53	0.8	0.48	0.95	0.94

[(ANOVA), factors being: timepoint—before or after endoscope insertion—and group healthy or lavaged] was computed to assess the significance of the difference in *C* among the groups: For all PEEP levels, *C* was significantly higher in the healthy group compared to the lavage group. A pressure-related increase of relative alveolar area $\Delta A(p_{\text{Tip}}) = (0.56 \pm 0.33)\%/mbar$ was found by analyzing data of 150 alveoli (each in 200 images) from two representative animals.

4 Discussion

We evaluate the invasiveness of a new method for intravital microscopy of subpleural alveoli. The method is based on endoscopic microscopy that we introduced for *in vivo* characterization of mechanical tissue properties and that we used for analyzing alveolar mechanics in a rat model under mechanical ventilation.⁴ Using this method, the thorax and the endoscopic system together build an air-sealed system where the lung was slightly fixated by application of a small negative pressure. By enhancing an endoscope with a trocar- and pressure-controlling-system, we were able to continuously record images of focused subpleural alveoli with a minimally opened thorax in the otherwise intact animal. Thereby, in the rat model, the respiratory system mechanics were only slightly changed and mean arterial pressure and *paO*₂ remained unchanged indicating minimal physiological stress.

To the authors' knowledge, the presented technique is the first allowing the continuously focused recording of subpleural alveoli without requiring surgical removal of large parts of the thoracic wall. The main results of this study support our hypothesis that the minimal invasiveness and the possibility to record focused images even while the lung is mechanically ventilated are the main advantages over existing methods.

The results of FE model I indicated that the pressure in the field of view is distributed homogeneously. The pressure difference between center and periphery was $<2\%$. Such small differences are likely negligible when analyzing the mechanical or morphological behavior of the recorded subpleural alveoli.

The influence of the negative pressure on the observed alveoli was evaluated in theory using FE model II and by *in vivo* measurements of size increase of visible alveoli reasoned by suction

pressure. Both evaluations indicated that the influence on the observed tissue reasoned by the negative pressure is small. Results from the FE model show why: The stress is distributed among the inside of the lung tissue. The influence on the subpleural alveoli in the field of view is hence comparatively low⁹ at an average negative pressure being as low as -3 mbar. Recorded alveoli are therefore assumed to behave in their natural way. However, local lung damage caused by the introduced endoscope cannot be completely ruled out because, according to FE model II, the stress at the border of the included area where the trocar contacts the parenchyma is higher than the applied negative pressure.

The purpose of our *in vivo* experiments in the rat model was to evaluate possible physiological influences of the endoscope's insertion on healthy and injured animals. Although the *paO*₂ was not significantly influenced in response to the endoscope's insertion, the MAP dropped significantly (by 15%) in the lung-injured animals. In contrast, in healthy animals, MAP was not influenced by the endoscope's insertion. Compliance of the lung-injured animals did not change significantly, while at particular circumstances the compliance of the healthy animals was significantly reduced after endoscope insertion.

It has to be noted that, in order to increase methodological sensitivity on such influences, we did not correct the statistics for multiple comparisons. If we had done so, then only one comparison would have remained significant. Furthermore, it must be noted that we targeted with our approach primarily on visualizing lung parenchyma at mostly unchanged boundary conditions for the lungs (i.e., at a most intact thorax). In this context, the found compliance drop is in contrast to most other methods of alveolar microscopy where large parts of the thoracic wall are removed and compliance of the respiratory system rises significantly. In all cases, compliance in healthy animals dropped significantly less than it dropped by bronchoalveolar lavage. Hence, the damage to the lung reasoned by insertion of the endoscope is small compared to the damage induced by the lavage.

A limitation of the analysis of invasiveness of our endoscopic method is lack of histological examination of the tissue. A further limitation concerns the translatability of information

about alveolar morphology to humans due to differences in pleural structure between different species. Furthermore, it must be kept in mind that any interpretation of morphological information must consider the anatomical site of the endoscope's tip because there may be differences in alveolar morphology between the dependent and nondependent lung (e.g., reasoned by gravitation).¹⁰

Further investigation is needed to combine morphological and functional information about alveolar geometry and mechanics to better understand alveolar recruitment/derecruitment and alveolar inhomogeneity during mechanical ventilation. The next step must be the in-depth analysis of alveolar morphology in videos recorded by this endoscopic method with high temporal resolution and automated alveolar image processing.

5 Conclusion

We present a novel method for recording continuously focused subpleural alveoli at the *in vivo* animal model with intact thorax. The mechanical influence on observed alveoli is small, and the method's influence on the cardiovascular and respiratory system of the rat model is small enough to discern between healthy and injured lung. Because of its minimal invasiveness and the absence of interference with dynamic lung mechanics, the method is capable of delivering knowledge on the natural behavior of subpleural alveoli in the rat model as well as in models of larger animals.

Acknowledgments

This project was supported by the German Research Foundation (Deutsche Forschungsgemeinschaft) "Protective Artificial Respiration" Grant Nos. KO 1814/6-1, KO 1814/6-2, GU 561/6-1, and GU 561/6-2.

References

1. The ARDS Network, "Ventilation with lower tidal volumes as compared with traditional tidal volumes for acute lung injury and the acute respiratory distress syndrome," *New England J. Med.* **342**(18), 1301–1308 (2000).
2. J. Frank and M. Matthay, "Science review: mechanisms of ventilator-induced injury," *Crit. Care* **7**(3), 233–241 (2003).
3. D. Dreyfuss and G. Saumon, "Ventilator-induced lung injury: lessons from experimental studies," *Am. J. Resp. Crit. Care Med.* **157**(1), 294–323 (1998).
4. D. Schwenninger, S. Schumann, and J. Guttmann, "In vivo characterization of mechanical tissue properties of internal organs using endoscopic microscopy and inverse finite element analysis," *J. Biomech.* **44**(3), 487–493 (2010).
5. D. Carney, J. DiRocco, and G. Nieman, "Dynamic alveolar mechanics and ventilator-induced lung injury," *Crit. Care Med.* **33**(3 suppl), 122–128 (2005).
6. B. D. Daly, G. E. Parks, C. H. Edmonds, C. W. Hibbs, and J. C. Norman, "Dynamic alveolar mechanics as studied by videomicroscopy," *Resp. Physiol.* **24**(2), 217–232 (1975).
7. J. D. DiRocco, L. A. Pavone, D. E. Carney, C. J. Lutz, L. A. Gatto, S. K. Landas, and G. F. Nieman, "Dynamic alveolar mechanics in four models of lung injury," *Intens. Care Med.* **32**(1), 140–148 (2006).
8. M. Mertens, A. Tabuchi, S. Meissner, A. Krueger, K. Schirmann, U. Kertzschner, A. R. Pries, A. S. Slutsky, E. Koch, and W. M. Kuebler, "Alveolar dynamics in acute lung injury: heterogeneous distension rather than cyclic opening and collapse," *Critical Care Medicine* **37**(9), 2604–2611 (2009).
9. G. F. Nieman, C. E. Bredenberg, W. R. Clark, and N. R. West, "Alveolar function following surfactant deactivation," *J. Appl. Physiol.* **51**(4), 895–904 (1981).
10. L. Pavone, S. Albert, J. DiRocco, L. Gatto, and G. Nieman, "Alveolar instability caused by mechanical ventilation initially damages the nondependent normal lung," *Critical Care* **11**(5), R104 (2007).
11. H. J. Schiller, U. G. McCann, D. E. Carney, L. A. Gatto, J. M. Steinberg, and G. Nieman, "Altered alveolar mechanics in the acutely injured lung," *Crit. Care Med.* **29**(5), 1049–1055 (2001).
12. J. Bickenbach, R. Dembinski, M. Czaplak, S. Meissner, A. Tabuchi, M. Mertens, L. Knels, W. Schroeder, P. Pelosi, W. M. Kuebler, R. Rossaint, and R. Kuhlen, "Comparison of two in vivo microscopy techniques to visualize alveolar mechanics," *J. Clin. Monitor. Comput.* **23**(5), 323–332 (2009).
13. S. Meissner, L. Knels, A. Krueger, T. Koch, and E. Koch, "Simultaneous three-dimensional optical coherence tomography and intravital microscopy for imaging subpleural pulmonary alveoli in isolated rabbit lungs," *J. Biomed. Opt.* **14**(5), 054020 (2009).
14. A. Tabuchi, M. Mertens, H. Kuppe, A. R. Pries, and W. M. Kuebler, "Intravital microscopy of the murine pulmonary microcirculation," *J. Appl. Physiol.* **104**(2), 338–346 (2008).
15. F. Chagnon, C. Fournier, P. G. Charette, L. Moleski, M. D. Payet, L. G. Dobbs, and O. Lesur, "In vivo intravital endoscopic confocal fluorescence microscopy of normal and acutely injured rat lungs," *Lab. Invest.* **90**(6), 824–834 (2010).
16. D. Schwenninger, K. Möller, H. Liu, and J. Guttmann, "Automated analysis of intratidal dynamics of alveolar geometry from microscopic endoscopy," *IEEE Trans. Biomed. Eng.* **57**(2), 415–421 (2010).
17. F. Suarez-Sipmann, S. H. Böhm, G. Tusman, T. Pesch, O. Thamm, H. Reissmann, A. Reske, A. Magnusson, and G. Hedenstierna, "Use of dynamic compliance for open lung positive end-expiratory pressure titration in an experimental study," *Crit. Care Med.* **35**(1), 214–221 (2007).
18. T. Luecke, J. P. Meinhardt, P. Herrmann, A. Weiss, M. Quintel, and P. Pelosi, "Oleic acid vs saline solution lung lavage-induced acute lung injury," *Chest* **130**(2), 392–401 (2006).
19. L. B. Ware and M. A. Matthay, "The acute respiratory distress syndrome," *New Eng. J. Med.* **342**(18), 1334–1349 (2000).